Scilight

Bioinorganics and Biocatalysis
https://www.sciltp.com/journals/bb

Article

Green Peptide-Assisted Synthesis of Gold Nanoparticles for Electrochemical Biosensing of Carbamate Pesticides

Marcos R. de Araujo Silva [1], Barbara B. Gerbelli [2], Ana Cristina H. de Castro-Kochi [1,3], Andrea M. Aguilar [4] and Wendel A. Alves [1,*]

[1] Centro de Ciências Naturais e Humanas, Universidade Federal do ABC, Santo André 09280-560, Brazil
[2] Diamond Light Source, Didcot OX11 0DE, UK
[3] School of Biomedical Engineering, Einstein Hospital Israelita, São Paulo 05521-200, Brazil
[4] Instituto de Ciências Ambientais, Químicas e Farmacêuticas, Universidade Federal de São Paulo, Diadema 09972-270, Brazil
* Correspondence: wendel.alves@ufabc.edu.br

How To Cite: de Araujo Silva, M.R.; Gerbelli, B.B.; de Castro-Kochi, A.C.H.; et al. Green Peptide-Assisted Synthesis of Gold Nanoparticles for Electrochemical Biosensing of Carbamate Pesticides. *Bioinorganics and Biocatalysis* **2026**, *1*(1), 4.

Summary of Figures and Tables

Figure S1. Schematic representation of the Fmoc solid-phase peptide synthesis route used to obtain the cysteine–diphenylalanine (CFF) tripeptide, including coupling, deprotection, and cleavage steps.

Figure S2. HPLC-MS characterization of the synthesized CFF peptide, showing (**a**) the chromatographic profile with a single dominant peak and (**b**) the ESI-MS spectrum confirming the expected molecular mass and high purity.

Figure S3. Atomic force microscopy (AFM) images of (**a**) CFF@AuNPs and (**b**) CFF peptide films, highlighting differences in nanoscale morphology and supramolecular organization.

Figure S4. High-resolution XPS spectra of the CFF peptide, showing the characteristic bonding environments of carbon (C 1s), oxygen (O 1s), and nitrogen (N 1s), consistent with the peptide backbone and side-chain functionalities.

Figure S5. (**a**,**c**,**e**) Cyclic voltammograms recorded at scan rates from 10 to 200 mV s^{-1} in 5.0 mM $[Fe(CN)_6]^{3-/4-}$ (100 mM sodium phosphate buffer, pH 7.0) for (**a**) bare SPE, (**c**) CFF peptide-modified SPE, and (**e**) CFF@AuNPs-modified SPE. (**b**,**d**,**f**) Corresponding plots of anodic and cathodic peak currents (i_p) as a function of the square root of the scan rate ($v^{1/2}$) for (**b**) bare SPE, (**d**) CFF peptide-modified SPE, and (**f**) CFF@AuNPs-modified SPE, indicating diffusion-controlled electrochemical behavior.

Figure S6. Laviron plots of anodic and cathodic peak potentials (E_{pa} and E_{pc}) as a function of log v for (**a**) bare SPE, (**b**) CFF peptide-modified SPE, and (**c**) CFF@AuNPs-modified SPE, used to extract the charge-transfer coefficient (α) and the heterogeneous electron-transfer rate constant (k_0).

Table S1. Charge-transfer coefficient (α) and heterogeneous electron-transfer rate constant (k_0) obtained from Laviron analysis for bare and modified SPEs, summarizing the kinetic enhancement induced by the CFF@AuNPs nanostructured interface.

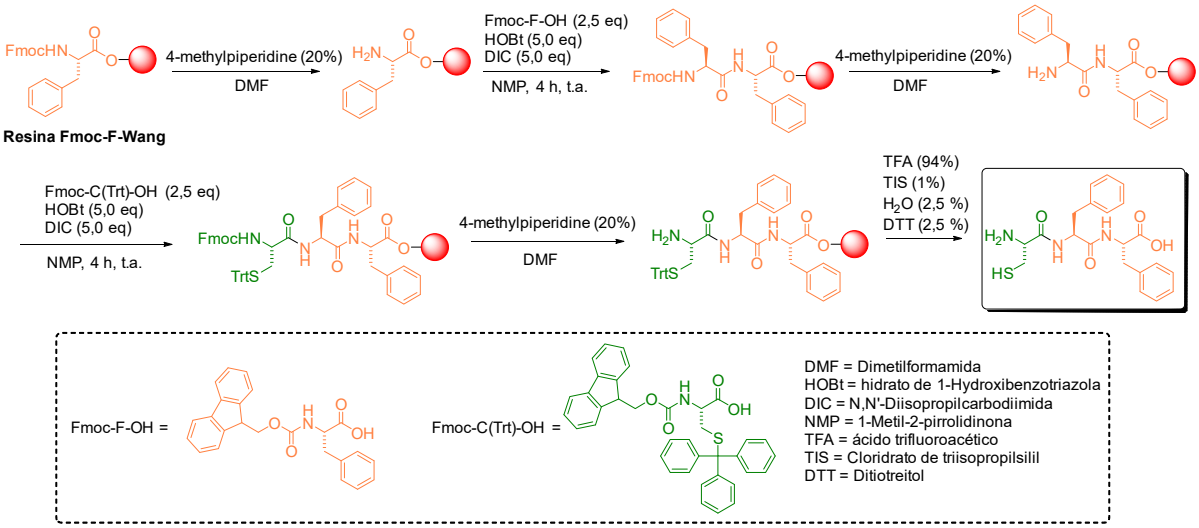

Figure S1. Schematic representation of the Fmoc solid-phase peptide synthesis route for the tripeptide CFF using Wang resin as solid support. The sequential coupling of Fmoc-protected phenylalanine and cysteine was carried out in the presence of *N*,*N*′-diisopropylcarbodiimide (DIC) and 1-hydroxybenzotriazole (HOBt), followed by Fmoc deprotection with 20% 4-methylpiperidine in DMF. Final cleavage and deprotection were achieved using a TFA/H_2O/DTT/TIS cocktail, yielding purified tripeptide CFF.

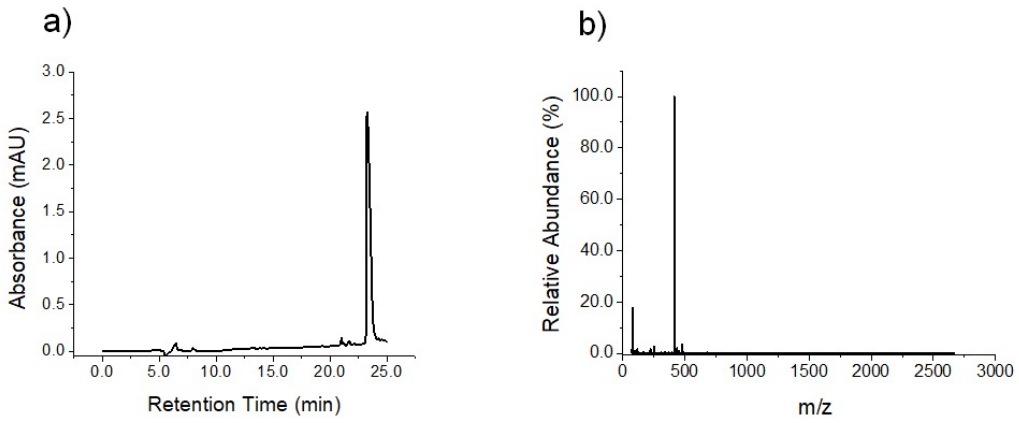

Figure S2. Characterization of the synthesized cysteine–diphenylalanine (CFF) peptide by HPLC–MS. (**a**) Chromatogram showing a single, well-defined peak at approximately 23 min, indicating high product purity. (**b**) ESI–MS spectrum in positive ion mode showing the characteristic molecular ion peak at m/z 416.2 ($[M + H]^+$) with a relative abundance of 99.98%, confirming the expected molecular structure of CFF.

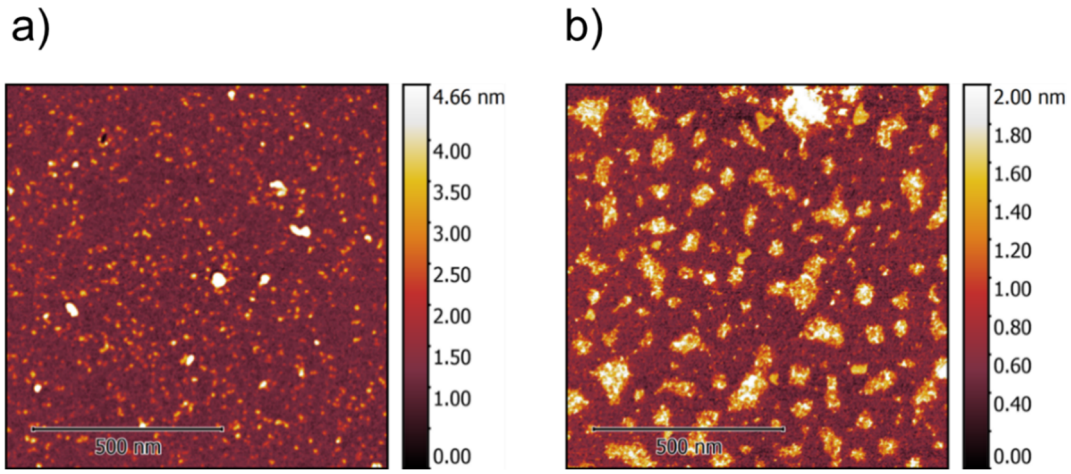

Figure S3. Atomic force microscopy (AFM) images showing the topography (**a**) CFF@AuNPs and (**b**) CFF peptide, highlighting differences in nanoscale organization and surface features.

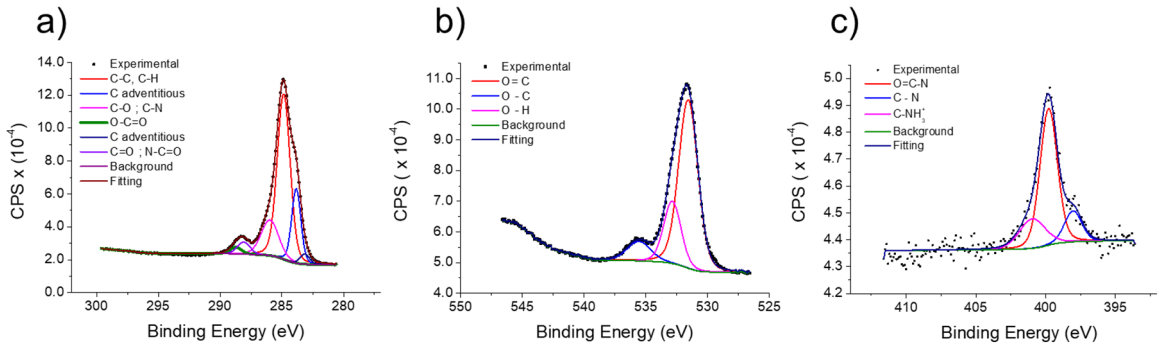

Figure S4. High-resolution XPS spectra of the CFF peptide highlighting the characteristic bonding environments of (**a**) carbon (C 1s), (**b**) oxygen (O 1s), and (**c**) nitrogen (N 1s), consistent with the peptide backbone and side-chain functionalities.

Determination of the Heterogeneous Electron-Transfer Rate Constant (k_0):

The heterogeneous electron-transfer rate constant (k_0) was determined using Laviron's method, which is suitable for quasi-reversible electron-transfer processes occurring at surface-modified electrodes. CVs were recorded for the reversible $[Fe(CN)_6]^{3-/4-}$ redox couple (5.0 mM in 100 mM sodium phosphate buffer, pH 7.0) at scan rates ranging from 10 to 200 mV s^{-1} for bare screen-printed carbon electrodes (SPEs) and for electrodes modified with CFF@AuNPs.

Representative CVs obtained at different scan rates are shown in Figure S5. As the scan rate increased, systematic shifts of the anodic (E_{pa}) and cathodic (E_{pc}) peak potentials were observed, indicating deviation from ideal reversible behavior and justifying the application of Laviron's formalism.

For each electrode, the anodic and cathodic peak potentials were plotted as a function of log v (v = scan rate). The resulting Laviron plots are presented in Figure S6. In the high-scan-rate region, linear relationships between E_{pa}, E_{pc}, and log v were obtained, confirming the quasi-reversible electron-transfer regime.

According to Laviron's theory, the slopes of the linear regions are related to the charge-transfer coefficient (α) by:

$$slope_{anodic} = \frac{2.303\,RT}{(1-\alpha)nF} \quad and \quad slope_{cathodic} = -\frac{2.303\,RT}{\alpha nF}$$

where R is the gas constant, T is the absolute temperature, F is the Faraday constant, and n is the number of electrons transferred (n = 1 for the $[Fe(CN)_6]^{3-/4-}$ redox couple). The values of α were extracted from the slopes of the anodic and cathodic branches.

Once α was determined, the apparent heterogeneous electron-transfer rate constant (k_0) was calculated from the intercepts of the Laviron plots using:

$$E_p = E^0 + \left(\frac{2.303\,RT}{\alpha nF}\right) \log\left(\frac{RTk_0}{\alpha nF}\right) + \left(\frac{2.303\,RT}{\alpha nF}\right) \log v$$

where E^0 is the formal potential of the redox couple. All symbols have their conventional electrochemical meanings.

The calculated values of α and k_0 for bare and modified electrodes are summarized in Table S1. The modification of the electrode surface with CFF-stabilized gold nanoparticles resulted in a pronounced increase in k_0 compared to the bare SPE, indicating enhanced interfacial electron-transfer kinetics induced by the nanostructured peptide–AuNP layer. These kinetic parameters are fully consistent with the trends observed in the cyclic voltammetry and electrochemical impedance spectroscopy measurements discussed in the main text.

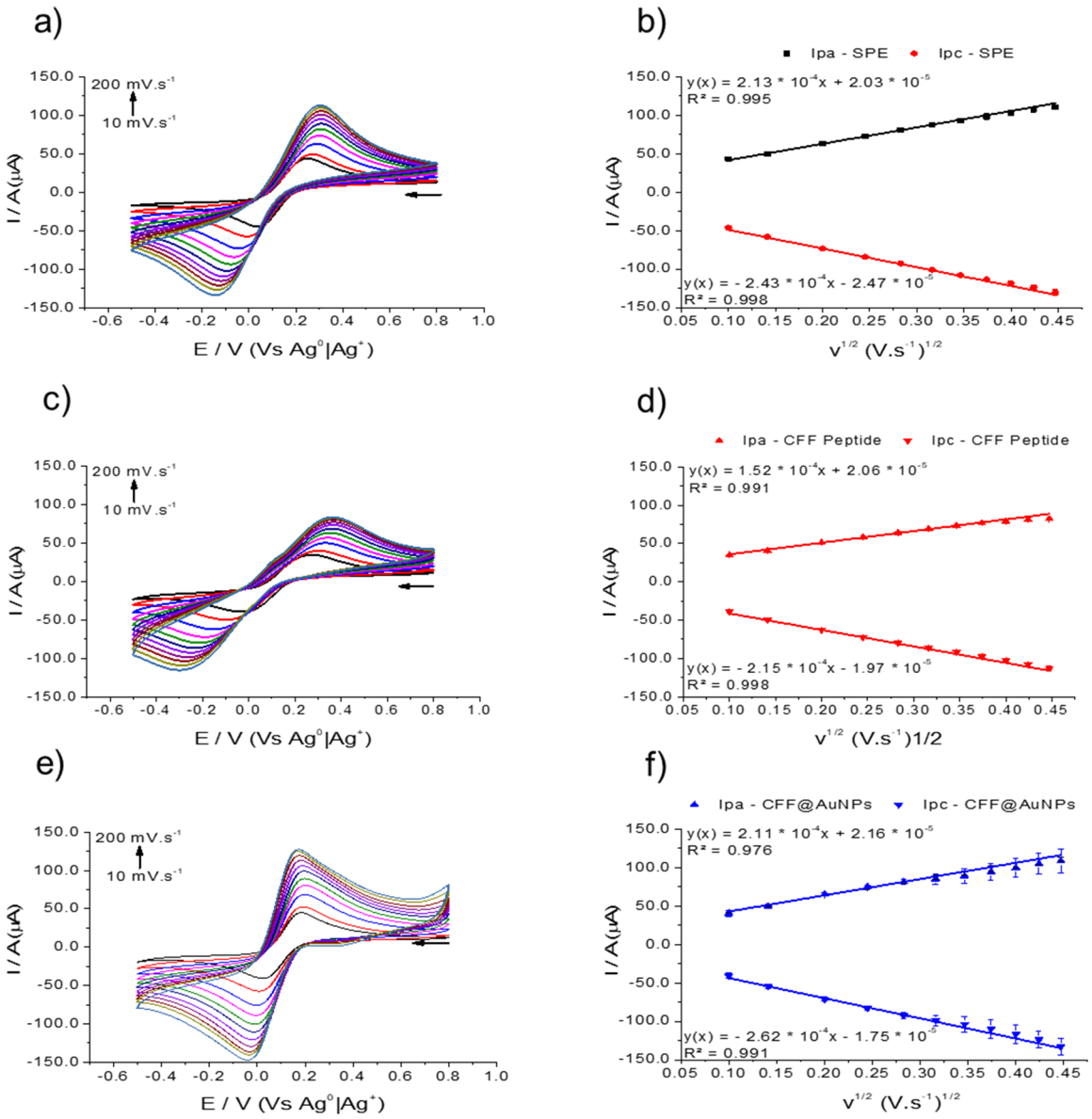

Figure S5. (**a**,**c**,**e**) Cyclic voltammograms recorded at scan rates from 10 to 200 mV s^{-1} in 5.0 mM $[Fe(CN)_6]^{3-/4-}$ (100 mM sodium phosphate buffer, pH 7.0) for (**a**) bare SPE, (**c**) CFF peptide-modified SPE, and (**e**) CFF@AuNPs-modified SPE. (**b**,**d**,**f**) Corresponding plots of anodic and cathodic peak currents (i_p) as a function of the square root of the scan rate ($v^{1/2}$) for (**b**) bare SPE, (**d**) CFF peptide-modified SPE, and (**f**) CFF@AuNPs-modified SPE, indicating diffusion-controlled electrochemical behavior.

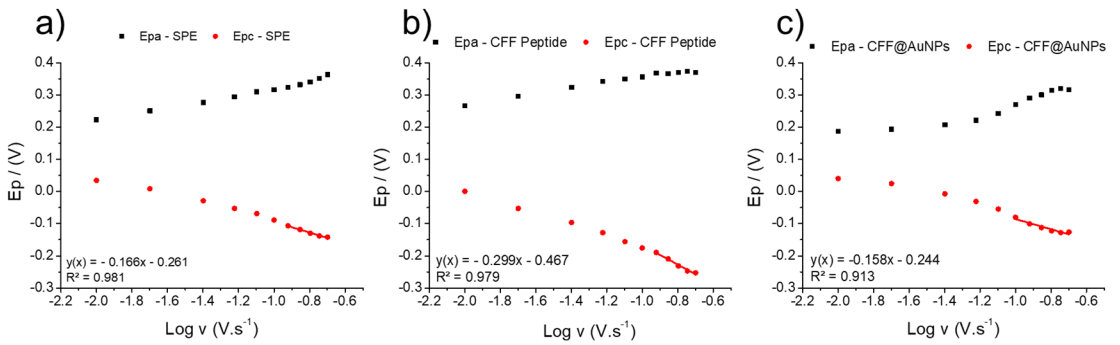

Figure S6. Laviron plots of anodic and cathodic peak potentials (E_{pa} and E_{pc}) as a function of log v for (**a**) bare SPE, (**b**) CFF peptide-modified SPE, and (**c**) CFF@AuNPs-modified SPE, used to extract the charge-transfer coefficient (α) and the heterogeneous electron-transfer rate constant (k_0).

Table S1. Charge-transfer coefficient (α) and heterogeneous electron-transfer rate constant (k_0) obtained from Laviron analysis for bare and modified screen-printed carbon electrodes.

Electrode	α (-)	k_0 (s^{-1})
SPE	0.37 ± 0.01	0.04 ± 0.01
SPE + CFF Peptide	0.32 ± 0.01	0.02 ± 0.01
SPE + [CFF@AuNPs]	0.67 ± 0.04	0.25 ± 0.05

Values were obtained from Laviron's analysis of cyclic voltammograms recorded at scan rates from 10 to 200 mV s^{-1} in 5.0 mM $[Fe(CN)_6]^{3-/4-}$ (100 mM phosphate buffer, pH 7.0). Data represent mean ± standard deviation (n = 3).